

# Metal-nonmetal transition of lanthanum hydrides, analyzed by $^{139}\text{La}$ hyperfine interaction

S. Leyer, S. Heck, A. Kaiser, and E. Dormann\*

Physikalisches Institut, Universität Karlsruhe, D-76128 Karlsruhe, Germany

R. G. Barnes

Department of Physics and Ames Laboratory, U.S. Department of Energy, Iowa State University, Ames, Iowa 50011, USA

(Received 23 March 2005; revised manuscript received 1 July 2005; published 20 September 2005)

Lanthanum hydrides  $\text{LaH}_x$ ,  $2.0 \leq x \leq 3.0$ , are characterized by static magnetic susceptibility analysis and  $^{139}\text{La}$  nuclear magnetic resonance investigations (line splittings, linewidth, line shift, and spin lattice relaxation). Temperature and composition dependence of all quantities is determined. Chemical shift is larger than the Knight shift for  $^{139}\text{La}$  in the  $\text{LaH}_x$  compounds. The  $x$  dependence of the density of states  $D(E_F)$  is derived site selectively and separated into  $s$ - and  $d$ -like contributions.

DOI: 10.1103/PhysRevB.72.125115

PACS number(s): 71.30.+h, 76.60.Cq, 76.60.Es, 75.20.-g

## I. INTRODUCTION

This contribution is focused on the metal-nonmetal transition of lanthanum hydrides.<sup>1-3</sup> Lanthanum dihydride ( $\text{LaH}_2$ ) is a metal ( $M$ ) with usual reflectivity for visible light. Superconductivity, with  $T_{sc}=0.17$  K was mentioned for  $\text{LaH}_{2.10}$ .<sup>4</sup> Lanthanum trihydride  $\text{LaH}_3$  is an optically transparent nonmetal ( $I$ ). The  $M$ - $I$  transition of lanthanum hydrides  $\text{LaH}_x$  was already reported 50 years ago.<sup>5,6</sup> Nevertheless, many questions of this  $M$ - $I$  transition are still unclear, in spite of the fascinating reversible electrochemical switching phenomena of thin films of rare-earth hydrides  $\text{RH}_x$  or  $\text{YH}_x$  between optical transparency and high reflectivity, reported and studied recently.<sup>7,8</sup> How important is the role of electron correlations and of atomic order?<sup>9-10</sup> Is  $x_c \approx 2.86$  the critical concentration for the  $M$ - $I$  transition in  $\text{LaH}_x$  as concluded from radiofrequency damping ( $Q$ -factor) measurements?<sup>11</sup> Is there a difference in the H concentrations  $x_c$  for the disappearance of the density of states at the Fermi surface for the H sites  $x_c(\text{H})$  and the La sites  $x_c(\text{La})$  in  $\text{LaH}_x$ ?<sup>12</sup> These questions will be tackled with the extensive  $^{139}\text{La}$  nuclear magnetic resonance (NMR) investigations presented below.

At first glance, in an ionic picture, assuming hydrogen enters as  $\text{H}^-$  and lanthanum as  $\text{La}^{3+}$ , the  $M$ - $I$  transition from metallic  $\text{LaH}_2$  with one conduction electron per formula unit to nonmetallic  $\text{LaH}_3$  seems straightforward.<sup>1-3</sup>  $(3-x)$  conduction electrons per formula unit  $\text{LaH}_x$  would give a variation of the density of states  $D(E_F)$  with  $(3-x)^{1/3}$  in the free electron picture. In fact, the  $\text{Gd}^{3+}$  impurity ion  $4f$  electron spin Korringa relaxation rate is consistent with a variation of the  $D(E_F)$  as  $(2.91-x)^{1/3}$ ,<sup>12</sup> suggesting that the metallic state is not supported beyond  $x=2.91$ . Proton spin lattice relaxation also appears to roughly support this picture.<sup>3,12,13</sup> The actual electronic band structure must be more complicated, however, because starting from  $\text{LaH}_2$ , with the cubic  $\text{CaF}_2$  crystal structure [with a face centered cubic lanthanum sublattice and all tetrahedral ( $t$ ) sites occupied by H], for  $2.0 < x \leq 3.0$  the octahedral ( $o$ ) interstitial sites are filled with hydrogen. Nevertheless, an overall lattice contraction is observed.<sup>6</sup> Evidently, the local La surroundings can not be cubic for  $2 < x < 3$ , thus, e.g., electric field gradients at the

$^{139}\text{La}$  nucleus have to be expected and were observed,<sup>3,13-15</sup> and integral measurements can reflect only an averaged density of states.

A roughly linear, instead of the 1/3-power variation, of the integral density of states  $D_\gamma(x)$  with hydrogen concentration  $x$  was derived in heat capacity studies for  $\text{LaH}_x$  or  $\text{LaD}_x$ .<sup>4,16-18</sup> The absolute value of  $D_\gamma(E_F)$  is small, even for  $\text{LaH}_2$  (Fig. 1). Since the published transition temperature to superconductivity  $T_{sc}=0.17$  K, of the dihydride is small,<sup>4</sup> only a minor correction of  $D_\gamma(E_F)$  for electron phonon coupling is expected.<sup>9</sup> Thus a bare density of states of  $D_0(E_F) \approx 0.91/\text{eV}$ , formula unit (f.u.), and both spins is obtained for  $x \approx 2.4$ .<sup>9</sup> Several  $x$  ranges, i.e.,  $1.9 < x < 2.2$ ,  $2.2 < x < 2.45$ ,  $2.45 < x < 2.6$ , and  $2.6 < x < 2.9$ , had to be distinguished in the specific heat analysis, and pronounced thermal anomalies in the 270–200 K range were related to hydrogen ordering transitions and superstructure formations.<sup>4,10</sup> Low-temperature tetragonal distortion of the cubic  $\text{LaH}_x$  structure was also reported for  $2.15 \leq x \leq 2.55$  and  $2.7 \leq x \leq 2.8$  from x-ray structural analysis.<sup>19</sup> Neutron-powder diffraction for  $\text{LaD}_{2.25}$  revealed the onset of long-range order in the sublattice of the octahedral interstices already at temperatures be-

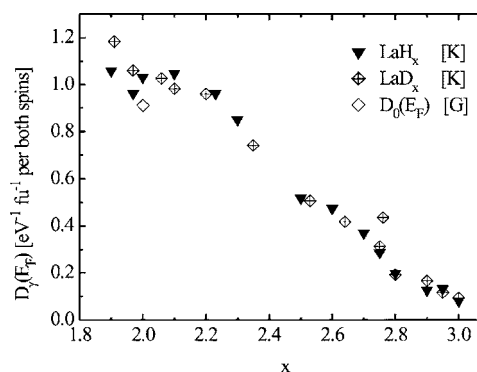


FIG. 1. Density of states  $D_\gamma(E_F)$  for both spin directions, per formula unit  $\text{LaH}_x$  and 1 eV versus hydrogen concentration  $x$ , derived from electronic contribution to specific heat. The bare value  $D_0(E_F)$ , corrected for electron phonon interaction, is included for  $\text{LaH}_{2.10}/\text{LaH}_{2.01}$ . See text for details. Data references [K]: Ref. 4, [G]: Refs. 4 and 9.

low 345 K.<sup>20</sup> In LaD<sub>2.50</sub> long-range ordering of the *o*-site sublattice, setting on at the tetragonal distortion at about 385 K, is "... complete by about 250 K and can be described as a repeating sequence of four (042) *o*-site planes comprised of two adjacent filled planes followed by two adjacent empty planes."<sup>21,22</sup>

The most puzzling experimental observation of the previous LaH<sub>*x*</sub> studies is the apparently only weak dependence of the presumed <sup>139</sup>La Knight shift on hydrogen concentration in LaH<sub>*x*</sub>.<sup>13,14,23</sup> In contrast to the <sup>1</sup>H or <sup>2</sup>D NMR studies that aimed primarily at the analysis of the hydrogen hopping motion,<sup>3,24</sup> but gave H-site density of states information via the Korringa relaxation contribution of the conduction electrons to the proton spin lattice relaxation,<sup>3,12</sup> the <sup>139</sup>La NMR studies had to struggle with the quadrupolar broadening of the *I*=7/2 nucleus' resonance lines.<sup>15,25</sup> Thus the motional narrowing of the NMR line in the high temperature (fast H hopping) range had to be used, in order to derive the H-concentration dependence of the <sup>139</sup>La Knight shift.<sup>13,14,23</sup> The resonance line shift with respect to LaCl<sub>3</sub> in aqueous solution decreases by barely a factor of 2 from +0.23% for *x*=2.0 to +0.12% for *x*=2.86 and is constant for *x*>2.86.<sup>12,13</sup> If this line shift is interpreted as the <sup>139</sup>La Knight shift, evidently a remaining density of states even for *x*>2.86 has to be claimed for the La site. However, using Gd<sup>3+</sup> 4*f* electron spin Korringa relaxation as a local conduction electron density probe, a decrease of the La-site specific density of states by at least a factor of 3 for 2.0 ≤ *x* ≤ 2.87 was demonstrated recently.<sup>12,26</sup> Thus, the presently available experimental results concerning integral or site specific conduction electron density of state *D*(*E*<sub>*F*</sub>) must be assessed as contradictory.

With the detailed static and dynamic magnetic investigations reported below, we analyze the metal-nonmetal transition of lanthanum hydrides, from the integral as well as from a local point of view. Important experimental details are explained in Sec. II. The results of static magnetic susceptibility measurements and the various consequences of the hyperfine interaction of the <sup>139</sup>La nucleus (*I*=7/2, 99.9% abundancy) are presented in Sec. III.

The first question that will be tackled with the current analysis is the evidence for electron-electron correlations in LaH<sub>*x*</sub>. The straightforward comparison between *D*<sub>*γ*</sub>(*E*<sub>*F*</sub>), the density of states at the Fermi level accessible by specific heat measurement (Fig. 1), which is modified only by electron-phonon interaction, and *D*<sub>*χ*</sub>(*E*<sub>*F*</sub>), the corresponding information obtained from Pauli paramagnetism, calculated via static magnetic susceptibility analysis (Sec. III A), which is enhanced by electron-electron interaction, will be discussed in Sec. IV A. Indeed, the value of about 2.5 of the Wilson ratio  $R = (\chi/\gamma)(\pi^2 k_B^2/3\mu_0\mu_B^2)$ , or of *D*<sub>*χ*</sub>(*E*<sub>*F*</sub>)/*D*<sub>*γ*</sub>(*E*<sub>*F*</sub>), which is also typically found in heavy fermion systems,<sup>27</sup> is determined for the LaH<sub>*x*</sub> compounds. We point, however, to the fact that also an induced orbital or van Vleck contribution to the paramagnetic susceptibility can explain this enhancement.

The second, more puzzling question is solved by the very detailed <sup>139</sup>La NMR analysis of the local density of states at the rare earth site in LaH<sub>*x*</sub>. We show that the apparent problem of the only weakly *x*-dependent density of states for increasing H concentration, resulting from only halving of

the <sup>139</sup>La-NMR line shift with respect to an aqueous solution of LaCl<sub>3</sub>, when going from LaH<sub>2</sub> to LaH<sub>3</sub>,<sup>12,23</sup> has been eliminated. The respective experimental results are presented in Secs. III B and III E. They are discussed in Sec. IV B. Spin-lattice relaxation turns out to be the reliable information source.<sup>28</sup> The conclusions (Sec. V) summarize the remarkable progress achieved with the current <sup>139</sup>La NMR analysis in the quantitative monitoring of the *x*-dependent La-site density of states at the LaH<sub>*x*</sub>-*M-I* transition.

## II. EXPERIMENTAL DETAILS

### A. Sample preparation

The powder samples were prepared at the Materials Preparation Center of Ames Laboratory, Iowa State University, from highest purity lanthanum (99.97 to 99.997 %). According to laser source mass spectrometric analysis, <20 (to <0.6) ppm Ce, <10 (to <0.2) ppm Gd, and 33 (to <0.08) ppm Yb are the highest amounts of rare earth impurities. A hardened steel mortar and pestle were used to grind the fragments down to approximately 40 μm size. Part of the samples were those used in earlier NMR studies.<sup>3,14,26,28,29</sup> The stoichiometry was analyzed twice and given to an error bar of ±0.015. For the NMR relaxation measurements, the powder samples were sealed in quartz ampoules of 6 mm diameter.

### B. Static magnetic susceptibility measurements

The static magnetic properties were derived with a Quantum Design MPMS SQUID magnetometer, with the powder samples surrounded by helium atmosphere during the measurements. Various field strengths between 0.1 and 50 kOe were applied, and temperature was varied between 2 and 300 K. The raw data of the field- and temperature-dependent magnetic moments *m*(*H*, *T*) had to be corrected for a small content of a magnetically ordered impurity phase estimated to range between 62 and 539 μg Fe per 1 g of the various lanthanum hydride samples, not inconsistent with the sample preparation procedure (Table I). To separate the temperature independent magnetic susceptibility from ferromagnetic and Curie paramagnetic defect contributions, the slopes of

$$m(H, T) \frac{T}{H} = \left( m_{fm} + \chi H + \frac{CH}{T} \right) \frac{T}{H} = (m_{fm}/H + \chi)T + C \quad (1)$$

versus *T* were derived and extrapolated for 1/*H* → 0.

### C. Nuclear magnetic resonance measurements

A Bruker MSL 300 spectrometer with commercial and home-built probe heads, variable temperature gas flow cryostats using liquid helium or liquid nitrogen as coolant and magnetic field of about 70 kOe of a superconducting magnet were used for the <sup>139</sup>La NMR at about 42.45 MHz. Broad <sup>139</sup>La NMR spectra were recorded with varied frequency, while central line narrowing was achieved by magic angle spinning with rotation frequency up to 15 kHz.<sup>30</sup> The NMR spectra were obtained by Fourier transformation of the free

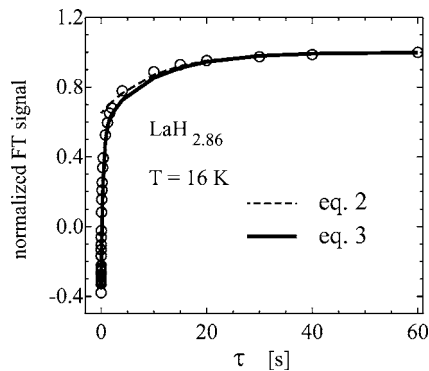


FIG. 2. Example of inversion recovery of the  $^{139}\text{La}$  central NMR line signal for a lanthanum hydride ( $\text{LaH}_{2.86}$ ,  $T=16$  K). The broken line shows the fit with a monoexponential function [Eq. (2)], the solid line a four-exponentials fit according to Eq. (3).

induction decay or of the second half of the spin echo in a  $90^\circ\text{-}\tau\text{-}180^\circ\text{-}\tau\text{-}$ spin echo sequence.  $\text{LaCl}_3$  in aqueous solution was used as  $^{139}\text{La}$ -NMR frequency standard as in earlier work.<sup>13,23</sup> To allow for an experimental estimate of the chemical shift contribution to the  $^{139}\text{La}$ -NMR line shifts in the various lanthanum hydrides, lanthanum diamagnetic compounds of varied electronegativity difference were analyzed as well.

An inversion-recovery spin-echo sequence with phase cycling was adopted for the measurements of the spin-lattice relaxation time. Due to the substantial  $^{139}\text{La}$  NMR line quadrupolar splitting and broadening, for the relaxation studies, in many cases only the central  $+1/2 \leftrightarrow -1/2$  transition could be analyzed. This gives rise to nonexponential signal recovery as exemplified in Fig. 2. Thus, instead of the result of Bloch's equations<sup>25</sup>

$$M(\tau) = M_0[1 - 2\exp(-\tau/T_1)], \quad (2)$$

the more general form (for  $I=7/2$ ,  $+1/2 \leftrightarrow -1/2$  transition) (Ref. 31)

$$M(\tau) \sim a_1 e^{-2W\tau} + a_2 e^{-12W\tau} + a_3 e^{-30W\tau} + a_4 e^{-56W\tau} \quad (3)$$

had to be fitted to the data. The  $T$  dependence of  $2W=T_1^{-1}$  for  $T < 80$  K was used for the derivation of the Korringa slope of the spin lattice relaxation rate.<sup>25</sup>

### III. RESULTS

#### A. Pauli paramagnetism

Stalinski reported already that the magnetic susceptibility is temperature independent in the lanthanum hydrides  $\text{LaH}_x$  ( $2 \leq x \leq 3$ ).<sup>5</sup> For the sample of dihydride  $\text{LaH}_{2.0}$  studied here the signatures of superconducting diamagnetic shielding at  $T < 4.5$  K (Fig. 3) are clearly more pronounced than expected for a compound with a transition temperature  $T_{sc}=0.17$  K that was reported for  $\text{LaH}_{2.10}$ .<sup>4</sup> This is probably not due to the lower impurity content of the sample studied here,<sup>32</sup> but can easier be explained by the contribution of less than 1% of La in this sample of  $\text{LaH}_2$ . Superconducting percolation with  $T_c \approx 6$  K due to cubic La has been observed

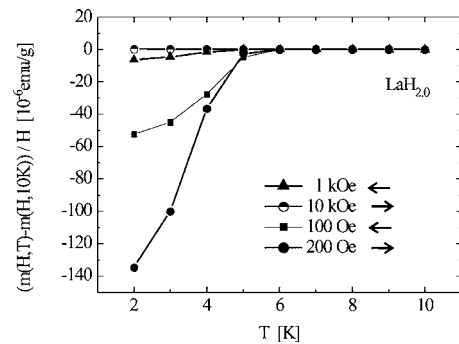


FIG. 3. Low-temperature diamagnetic contribution to magnetic susceptibility of  $\text{LaH}_{2.0}$ . These data were recorded within a sequence of cooling and heating runs for constant field strengths, varied always at the highest or lowest temperatures, respectively. This contribution can be explained by less than 1% La content of the  $\text{LaH}_2$  sample.

before in the system  $\text{LaH}_x$  for  $0 < x < 1.75$ , with a very small fraction of superconducting behavior remaining even for  $x=2$ .<sup>33</sup> The temperature independent part of the magnetic susceptibility of  $\text{LaH}_x$  was corrected for the core diamagnetism of  $\text{La}^{3+}$  ( $-20 \times 10^{-6}$  emu/mol), and, alternatively, for that of  $\text{H}^+$  or  $\text{H}^-$ , i.e., 0 or  $-1.6 \times 10^{-6}$  emu/mol.<sup>34</sup> The resulting values of the conduction electron paramagnetism  $\chi_p$  per mole of  $\text{LaH}_x$  are plotted in Fig. 4. Landau diamagnetism of the conduction electrons was not considered, on account of the predominant  $d$ -like character of the dihydride conduction electrons.<sup>8,35,36</sup> Figure 4 shows clearly that the conduction electron paramagnetic susceptibility  $\chi_p$  of the lanthanum hydrides decreases roughly linearly with increasing hydrogen content  $x$ , as was previously reported for the specific heat coefficient  $\gamma$  (Fig. 1).<sup>4</sup>

#### B. $^{139}\text{La}$ NMR line width

Compared to the cubic lanthanum dihydride  $\text{LaH}_{2.0}$ , severe line broadening of the central  $^{139}\text{La}$  NMR line is observed for  $\text{LaH}_x$  with  $2 < x < 3$ . The quadrupolar origin of

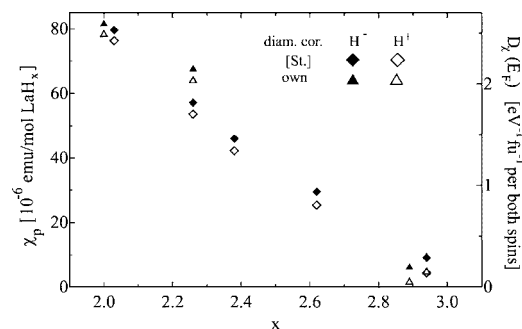


FIG. 4. Conduction electron paramagnetism and density of states of  $\text{LaH}_x$  versus hydrogen concentration  $x$ , calculated from static magnetic susceptibility under the assumption of the validity of Eq. (16) (own data and published results, St: Ref. 5), diamagnetic correction for  $\text{H}^-$  or  $\text{H}^+$ . The density of states  $D_x(E_F)$  is overestimated as a result of neglecting the contribution of van Vleck paramagnetism to  $\chi_p$ .

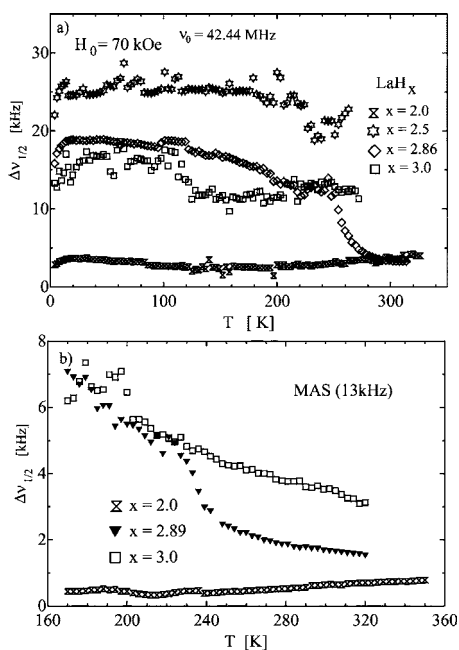


FIG. 5. Temperature dependence of central  $^{139}\text{La}$  NMR line width of different  $\text{LaH}_x$  samples ( $H_0 = 70$  kOe,  $\nu_0 = 42.45$  MHz,  $90^\circ$  pulse length varying between 1 and 4  $\mu\text{s}$ ). Upper part: Half width at half height, determined from Fourier transformed spin echo signal. For  $\text{LaH}_{2.5}$  only the central part of the inhomogeneously broadened  $+1/2 \leftrightarrow -1/2$  transition is excited under the experimental conditions. Lower part: Examples for the line narrowing by magic angle spinning, rotation frequency 13 kHz. Fourier transform of free induction decay signal.

this inhomogeneous line broadening has been reported before.<sup>13,15,23,28</sup> Figure 5 shows examples for the temperature dependence of the linewidth. The line narrowing in the high-temperature range is due to fast thermally activated proton hopping motion, as is typical for hydrides.<sup>3</sup> The largest width is not observed for the highest hydrogen concentration, with the largest influence of  $^{139}\text{La}$ - $^{139}\text{La}$  and  $^{139}\text{La}$ - $^1\text{H}$  nuclear dipolar interaction. Instead, the  $\text{LaH}_x$  compounds with  $x \approx 2.5$ , which show tetragonal distortion already above room temperature,<sup>19</sup> give rise to the width maximum via second order quadrupolar contribution. Under these conditions, even only a part of the inhomogeneously broadened  $+1/2 \leftrightarrow -1/2$  transition is measured. For the higher  $x$  range, hydrogen ordering in the 250 K range is discernible from line-width anomaly.

The lower part of Fig. 5 displays the line narrowing influence of magic angle spinning (MAS) for some of the  $\text{LaH}_x$  compounds.<sup>37</sup> Since the  $^{139}\text{La}$  NMR line shifts amount to 0.24% with respect to an aqueous solution of  $\text{LaCl}_3$  at most, which is 100 kHz at the measuring frequency of about 42.45 MHz, this line width reduction achievable by MAS techniques evidently is a must in order to reduce the error bar to an acceptable limit. Slowed-down motion and ordering of the H atoms ( $\text{H}^-$  ions) causes line broadening in  $\text{LaH}_{2.89}$  at  $T \approx 250$  K in spite of MAS line narrowing, due to the increased quadrupolar contribution, as is clearly visible in Fig. 5(b).

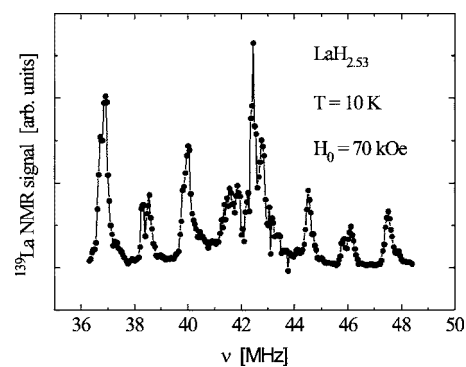


FIG. 6. Quadrupolar splitting of  $^{139}\text{La}$  NMR line in  $\text{LaH}_{2.53}$ . Typical spectrum, recorded by varying the frequency. [ $H_0 = 70$  kOe]  $T = 10$  K, 50 kHz steps, magnitude calculation of FT signal, rf power optimized, uncalibrated.] The six quadrupole satellites (edge singularities) and the second order quadrupolar broadened central line ( $\sim 1$  MHz) can be discerned. Additional narrow weak lines are visible in the central part.

### C. $^{139}\text{La}$ line splittings

Well-defined quadrupolar splitting was observed for the medium hydrogen concentration range  $x = 2.5 - 2.6$ . The tetragonal distortion of  $\text{LaH}_x$  compounds was reported in the phase diagram presented by Boroch *et al.*<sup>19</sup> and for  $2.6 \leq x \leq 2.86$  already earlier by Klavins *et al.*<sup>38</sup> Figure 6 shows one example of the quadrupolar splitting. This main spectrum shows only weak temperature dependence in the low-temperature range. In addition to the main spectrum, an additional spectrum with much smaller satellite line separation was observed, with relative intensity only in the percent range, and a presumably stronger temperature dependence.<sup>37</sup> These signals might also arise from sample oxidation or nitride formation during the NMR measurements.

The quadrupolar satellite lines for  $I = 7/2$ , originating from the  $(m-1) \rightarrow m$  transition, are observed at<sup>25</sup>

$$\nu = \nu_{Zee} + \frac{1}{2} \nu_Q (3 \cos^2 \vartheta - 1) \left( m - \frac{1}{2} \right) \quad (4)$$

in axially symmetric surrounding, with

$$\nu_{Zee}(x) = \nu_0 [1 + K(x) + \Delta\sigma(x)]. \quad (5)$$

The second order quadrupolar contribution to the “central” line ( $-1/2 \rightarrow +1/2$  transition) is given by

$$\nu_{1/2}^{(2)} = \frac{-\nu_Q^2}{16\nu_{Zee}} \left( I(I+1) - \frac{3}{4} \right) (1 - \cos^2 \vartheta) (9 \cos^2 \vartheta - 1). \quad (6)$$

Here,  $\nu_Q = 3e^2qQ/h2I(2I-1)$  is the quadrupolar splitting frequency parameter,  $\nu_0$  the Larmor frequency of the  $^{139}\text{La}$  frequency standard,  $K(x)$  and  $\Delta\sigma(x)$  the Knight shift and chemical shift difference for  $^{139}\text{La}$  in the respective  $\text{LaH}_x$  compound. The most prominent peaks of the quadrupolar satellites are observed at  $\vartheta = 90^\circ$ , thus their separation amounts to  $\Delta\nu_Q = \frac{1}{2} \nu_Q$ , only. From the  $\text{LaH}_{2.53}$  data shown in Fig. 6, we derive  $\Delta\nu_Q \approx 2$  MHz at 10 K, or twice this value for  $\nu_Q$ . This allows us to estimate the corresponding average

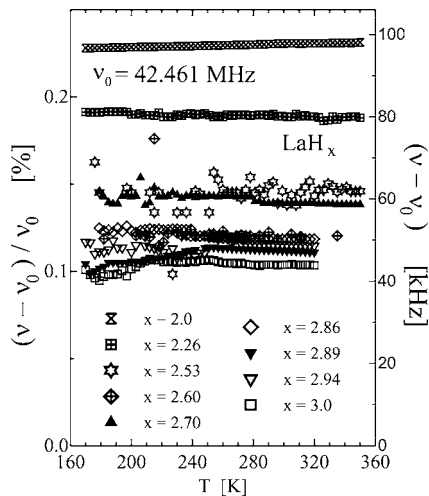


FIG. 7.  $^{139}\text{La}$  MAS-NMR line shift of various  $\text{LaH}_x$  samples versus temperature, in relative (absolute) units on left (right) hand scale, with  $\nu_0=42.461$  MHz of  $\text{LaCl}_3$  in aqueous solution. (For  $x=2.53$  and  $2.60$ , line shift may be reduced by the influence of quadrupolar interaction.)

central line shift due to the second order quadrupolar contribution

$$\overline{\delta\nu} = -\frac{1}{2} \frac{\nu_Q^2}{\nu_{Zee}}. \quad (7)$$

This amounts to  $-190$  kHz or  $-0.44\%$  at  $10$  K. This estimate demonstrates that a reliable low-temperature Knight shift analysis is rendered impossible in spite of the use of magic angle spinning, because the full second order quadrupolar width of the central line is  $5.2$  times as large, i.e., about  $1$  MHz, preventing any more detailed analysis. We would like to remind that magic angle spinning (with  $\vartheta_{\text{mag}}=54.74^\circ$ ) can reduce the second order quadrupolar contribution, but in order to eliminate it completely, additional spinning of the sample around a second axis ( $30.55^\circ$  or  $70.12^\circ$ ) would be required.<sup>39</sup> This feature is not available in our experimental setup.

It has to be emphasized that such prominent quadrupolar splitting of the  $^{139}\text{La}$  NMR lines could only be followed for the medium hydrogen concentrations  $2.5 \leq x \leq 2.6$ . The field gradients of the other compositions must be weaker, as was previously reported for  $x=2.38$  and  $2.74$ .<sup>15</sup> As is expected from the large number of possibilities to distribute  $n$  H atoms over six octahedral interstitial sites (i.e.,  $6!/[n! \cdot (6-n)!]$ ), it must vary strongly from one local La surrounding to the next. We have already shown the consequences on the central line width in Fig. 5. This is evidently rather favorable for the NMR analysis presented below

## D. $^{139}\text{La}$ NMR line shift

### 1. Lanthanum hydrides

Figure 7 shows the temperature dependence of the  $^{139}\text{La}$  NMR central line shift of the various  $\text{LaH}_x$  samples studied by magic angle spinning, referred to  $\text{LaCl}_3$  in aqueous solu-

tion as frequency standard ( $\nu_0=42.461$  MHz). There is substantial variation of the line shift ( $\nu - \nu_0$ ) with the hydrogen content  $x$  but only a minor temperature dependence. Actually, the obvious transition observed at  $T \approx 250$  K for  $\text{LaH}_{2.89}$  from  $T$ -independent high-temperature behavior, to  $T$ -dependent low-temperature behavior, is linked to the hydrogen disorder-order transition of this compound. This has been substantiated for the same compound by magnetic characterization of  $\text{Ce}^{3+}$  impurities before.<sup>26</sup> The observed  $T$ -dependent shift can be explained by the remnants of second order quadrupolar shift, Eq. (6), in spite of the magic angle spinning, because the linewidth increases in this temperature range [Fig. 5(b)]. A closer inspection of the  $x$ -dependent sequence of MAS-NMR line shift values ( $\nu - \nu_0$ ) reveals the influence of a remaining second order quadrupolar contribution especially for the  $x=2.53$  and  $2.60$  samples by their reduced shift values compared to the general  $x$ -dependent trend in Fig. 7.

It is tempting to relate  $(\nu - \nu_0)/\nu_0$  directly to the Knight shift  $K$  caused by the conduction electron hyperfine interaction with the  $^{139}\text{La}$  nucleus in the metallic hydrides, as was done in the early analyses,<sup>23,35</sup> yielding  $K \approx 0.23\%$  for  $\text{LaH}_2$ . In simple elemental metals with Knight shifts in the range up to  $1\%$  this approximation is acceptable. On the other hand, for  $\text{YH}_{1.99}$  the thus defined Knight shift of  $^{89}\text{Y}$  [measured by variable temperature  $^1\text{H} \rightarrow ^{89}\text{Y}$  cross polarization magic angle spinning (CP-MAS) NMR with respect to an aqueous solution of  $\text{YCl}_3$ ] amounted to only about  $940$  ppm.<sup>40</sup> It was pointed out that this value is only slightly larger than  $^{89}\text{Y}$  chemical shifts in nonmetals, ranging between  $+750$  and  $-200$  ppm.<sup>40,41</sup> Unfortunately, in the  $\text{LaH}_x$  compounds it is not possible to “switch off” the conduction electron density of states at the Fermi level just by varying the temperature, as can be done in organic metals subject to a Peierls metal-nonmetal transition.<sup>42</sup> We include the data derived in the present analysis in Table I as

$$(\nu - \nu_0)/\nu_0 = K + \Delta\sigma \quad (8)$$

because the shifts discussed here are by a factor  $2.8$ – $5.7$  smaller than the Knight shift of pure lanthanum metal. Therefore the chemical shift variation,  $\Delta\sigma$ , can have a considerable influence on the hydrogen concentration dependence of the line position.

### 2. Diamagnetic lanthanum compounds

The choice of an appropriate chemical shift standard for  $^{139}\text{La}$  Knight shift analysis in lanthanum hydrides is non-trivial. A solid with the same electronegativity ( $X$ ) difference and comparable coordination number seemed most reliable. Actually, because  $X_{\text{La}}=1.1$  and  $X_{\text{H}}=2.2$  (Allred-Rochow values<sup>43</sup>), comparison of  $\text{La}_2\text{O}_3$  ( $7$  coordinated,  $X_{\text{O}}=3.5$ ),  $\text{LaCl}_3$  ( $9$  coordinated,  $X_{\text{Cl}}=2.8$ ), and  $\text{LaI}_3$  ( $8$  coordinated,  $X_{\text{I}}=2.2$ ) points to  $\text{LaI}_3$  as a good choice for comparison with  $\text{LaH}_2$ , which has also eight nearest neighbors to La.<sup>44–46</sup> Table II compiles our results for the respective chemical shifts and the electronegativity differences.  $\Delta\sigma$  was derived by relating the peak position of the  $^{139}\text{La}$  lines of the solid compound to that of the liquid aqueous  $\text{LaCl}_3$  solution stan-

TABLE I. Relevant data of the investigated lanthanum hydrides. Estimated content of magnetically ordered magnetic impurities introduced by sample preparation techniques in second column,  $^{139}\text{La}$  NMR lineshift relative to the  $^{139}\text{La}$  NMR line of  $\text{LaCl}_3$  in aqueous solution: MAS,  $T \approx 300\text{--}305\text{ K}$  (line center,  $T=4\text{--}200\text{ K}$ ) (third column), relaxation-rate linear slopes  $[d/dT(T_1^{-1})=a]$  at 42.45 MHz (fourth column).  $a$  is unequivocally the Korringa slope for  $x \leq 2.87$ , but might be mixed up with the frequency dependent  $T$ -linear slope for the direct spin phonon relaxation process for  $x > 2.89$ .

Sample $\text{LaH}_x$	$\mu\text{g Fe}$ per g	$K+\Delta\sigma$ (%)	$a$ ( $10^{-3}\text{ s}^{-1}\text{K}^{-1}$ )
$\text{LaH}_{2.0}$	152	+0.230, (0.240)	82
$\text{LaH}_{2.26}$ :100 ppm Gd	539	+0.188	
$\text{LaH}_{2.35}$		(+0.219)	50
$\text{LaH}_{2.5}$		(+0.209)	19
$\text{LaH}_{2.53}$		+0.138	
$\text{LaH}_{2.6}$		+0.121, (0.164)	16.8
$\text{LaH}_{2.7}$		+0.139, (0.153)	16
$\text{LaH}_{2.84}$		(+0.134)	4.8
$\text{LaH}_{2.86}$		+0.118, (0.134)	6.3
$\text{LaH}_{2.87}$ :300 ppm Gd	321		
$\text{LaH}_{2.89}$	116	+0.111, (0.115)	1.5
$\text{LaH}_{2.89}$ :2700 ppm Ce	235		
$\text{LaH}_{2.92}$		(+0.124)	1.86
$\text{LaH}_{2.94}$	62	+0.115, (0.128)	1.66
$\text{LaH}_{3.0}$		+0.103, (0.120)	1.7

dard. Because the NMR lines of the solid samples had somewhat unsymmetrical wings, the separation of the respective centers of gravity  $\Delta\sigma_{CG}$  was calculated as well. The difference ( $\Delta\sigma - \Delta\sigma_{CG}$ ), given in Table II, may be used to estimate the reliability of  $\Delta\sigma$ .  $\Delta\sigma$  of all three solid compounds is comparable and quite different from that of the aqueous solution. Assuming  $\Delta\sigma(\text{LaH}_2) = +(0.21 - 0.18)\%$ , only  $K = +(0.03 - 0.06)\%$  is left for the conduction electron induced Knight shift in  $\text{LaH}_2$ . This absolute value is by a factor of 23–11 smaller than the Knight shift in La metal. No simple rule for the variation of  $\Delta\sigma$  with the hydrogen content, or with the coordination number of the La site in question (between 8 and 14) for  $x > 2.0$  can be given. Thus a reliable separation of  $K$  and  $\Delta\sigma$  for the hydrides  $\text{LaH}_x$  with

TABLE II. Chemical shift  $\Delta\sigma$  of diamagnetic solid  $^{139}\text{La}$  NMR standards with respect to an aqueous solution of  $\text{LaCl}_3$  ( $T = 293\text{ K}$ ). Abbreviations: La coordination number  $n$ , electronegativity of ligand  $X_{\text{Li}}$  (Ref. 43), chemical shift  $\Delta\sigma$ , and shift difference of line peaks and line centers of gravity ( $\Delta\sigma - \Delta\sigma_{CG}$ ), given as estimate of error limit.

	$n$	$X_{\text{Li}}$	$\Delta\sigma$ (%)	$(\Delta\sigma - \Delta\sigma_{CG})$ (%)
$\text{LaI}_3$	8	2.2	+0.210	+0.069
$\text{LaCl}_3$	9	2.8	+0.160	-0.019
$\text{La}_2\text{O}_3$	7	3.5	+0.184	+0.065

$x > 2.0$  is currently not possible. Their sum is given in Table I. These  $(K + \Delta\sigma)$  data compare reasonably with line shift results derived and discussed previously by other authors: Scaled with the outer electron hyperfine coupling constants,<sup>47</sup> the line shifts at the lanthanide site in the dihydrides  $\text{ScH}_2$ ,  $\text{YH}_2$ , and  $\text{LaH}_2$  fall in a narrow range of small positive values.<sup>35</sup> The  $^{89}\text{Y}$  line shift in  $\text{YD}_{2.98}$ ,  $(K + \Delta\sigma)_{\text{iso}} = 0.0361\%$ , on the other hand, was reported to fall in the middle of the range of chemical shifts for nonmetallic yttrium compounds.<sup>48</sup> In summary, all these line shift results are in agreement with a predominantly  $d$ -like density of states at the Fermi level for the rare-earth site,<sup>35</sup> with the absence of pronounced variation of the density of states around the Fermi level deduced from the absence of temperature dependence of  $(K + \Delta\sigma)$ .<sup>48</sup> The presence of a temperature independent additional van Vleck-type induced orbital contribution of susceptibility and line shift was proposed as well.<sup>35,36</sup>

### E. $^{139}\text{La}$ spin lattice relaxation

Under the conditions discussed in Sec. III D, spin lattice relaxation gives the more reliable estimate of the conduction electron density of states. Eventually, the Knight shift can then be calculated via the Korringa relation<sup>25</sup>

$$K^2 T_1^{ce} T = \frac{\hbar \gamma_{ce}^2}{4\pi k_B \gamma_{\text{La}}^2}, \quad (9)$$

at least as long as only one type of conduction electron comes into play. Different contributions to the  $^{139}\text{La}$  spin-lattice relaxation rate  $(T_1)^{-1}$  dominate in high- and low-temperature ranges. Generally

$$(T_1)^{-1} = (T_1)_{ce}^{-1} + (T_1)_{ho}^{-1} + (T_1)_{de}^{-1}. \quad (10)$$

Here

$$(T_1)_{ce}^{-1} = aT \quad (11)$$

is the Korringa relaxation caused by the hyperfine interaction with the conduction electrons, which predominates in the metallic hydrides at low temperature [Fig. 8(b)]. The fit parameters “ $a$ ” are compiled in Table I. The thermally activated hopping motion of the protons is responsible for the fast increase of  $(T_1)^{-1}$  at high temperature [Fig. 8(a)]. This contribution is a quadrupolar relaxation rate for the  $I=7/2$  nucleus, but may be approximately parametrized by<sup>49,50</sup>

$$(T_1)_{ho}^{-1} = A \frac{\tau_h}{1 + (\omega\tau_h)^2} \quad (12)$$

with

$$\tau_h = \tau_\infty \exp(Q/k_B T). \quad (13)$$

For the fit in Fig. 8(a), the activation energies  $Q$  derived in earlier work were used.<sup>24</sup> It is evident in Fig. 8(a) that the relaxation rate, at a fixed temperature, increases rapidly with decreasing  $x$  value for  $2.5 < x < 3.0$ , i.e., with increasing hydrogen vacancy concentration. This part is irrelevant for the low-temperature fit yielding the most relevant parameter “ $a$ .”

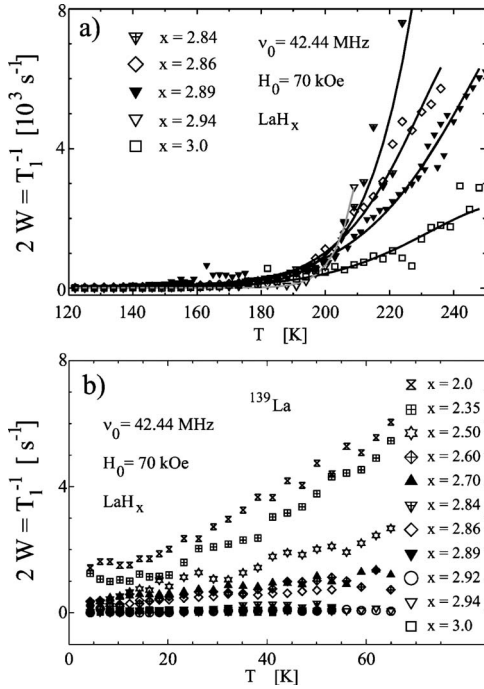


FIG. 8. Lanthanum spin lattice relaxation rate parameter  $2W = T_1^{-1}$  versus temperature of selected  $\text{LaH}_x$  samples (42.44 MHz, 70 kOe). High (a) and low temperature (b) range in upper and lower part, respectively. Solid lines are explained in text.

In the low- $T$  range, the various defects and impurities of the lanthanum hydrides, although of low concentration, have to be considered:<sup>26</sup>

$$(T_1)_{de}^{-1} = \frac{R}{[1 + (\omega_0\tau_c)^2]} + N\rho \left[ \frac{\tau_1}{1 + (\omega_0\tau_1)^2} \right]^p. \quad (14)$$

The first term is a  $T$ -independent,  $\omega_0^{-2}$ -dependent contribution caused, e.g., by the magnetically ordered defects, with very long  $\tau_c$ . The second term considers spin diffusion (in the cubic systems, such as  $\text{LaH}_{2.0}$ , with narrow  $^{139}\text{La}$  NMR line) to the very small, but not irrelevant concentration of paramagnetic defects [with electron spin relaxation time  $\tau_1(T)$ ,  $p \approx 0.95$  for  $\text{LaH}_{2.0}$ ].<sup>26</sup> Both contributions in Eq. (14) are small, but relevant for the error bar of the “ $a$ ” parameters (Table I).

Neglecting van Vleck susceptibility and orbital hyperfine interactions,<sup>47</sup> the Korringa slope “ $a$ ” is proportional to the square of the density of states  $D(E_F)$  and the square of the hyperfine coupling constant. Therefore, in Fig. 9 we plotted the square root of the parameter  $a$  versus hydrogen concentration  $x$  for all studied lanthanum hydrides  $\text{LaH}_x$ , reflecting the  $x$  dependence of the density of states. The similarity to the approximately linear variation of  $D_\gamma(E_F)$  versus  $x$  (Fig. 1) and  $\chi_p$  versus  $x$  (Fig. 4) is striking. The values of  $a^{1/2}$ , derived at 42.45 MHz, decrease according to Fig. 9 for  $\text{LaH}_x$  with  $x$  for  $2.0 \leq x \leq 3.0$  roughly linearly, may be except for plateaulike ranges for  $2.5 \leq x \leq 2.7$  and for  $2.89 \leq x \leq 3.0$ . For  $\text{LaH}_{2.87}$ :300 ppm Gd, we proved recently that the  $\text{Gd}^{3+}$  electron spin relaxes via Korringa relaxation.<sup>26</sup> For the La site of the lanthanum hydrides studied, the  $M$ - $I$  transition is

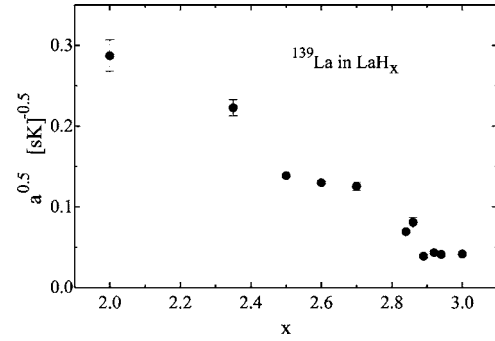


FIG. 9. Square root of the linear  $T$  dependent slope of the  $^{139}\text{La}$  low-temperature spin-lattice relaxation rate ( $\nu_0 = 42.44$  kOe), versus hydrogen content in  $\text{LaH}_x$ .

thus restricted to  $x_c > 2.87$ . From the relaxation measurements at only one fixed frequency ( $\nu_0 \approx 42.45$  MHz), experiment cannot discriminate between the Korringa relaxation [Eqs. (11) and (9)] caused by conduction electrons, or a direct spin-lattice relaxation process<sup>25,51</sup>

$$(T_1)_{\text{SL}}^{-1} = \alpha \nu_0^3 \coth\left(\frac{\hbar \nu_0}{2k_B T}\right) \quad (15)$$

because both of them give rise to a linear increase of  $(T_1)^{-1}$  with  $T$  in the temperature range studied. However, the Korringa relaxation rate is independent of the Larmor frequency, i.e.,  $a \neq f(\nu_0)$  in Eq. (11), whereas the latter one increases with  $\nu_0^2$ . The frequency independence of  $a$  proved the nonvanishing conduction electron density of states for  $x = 2.87$ .<sup>26</sup> Only for  $x \geq 2.89$  in Fig. 9 the contributions of Eqs. (11) and (15) might be mixed up. If all the residual values of  $a^{1/2}$  for  $2.89 \leq x \leq 3.0$  in Fig. 9, are ascribed to the direct process, Eq. (15), the critical concentration  $x_c$  at low temperatures would be taken to be  $2.91 \pm 0.02$ , consistent with the  $\text{Gd}^{3+}$  results.<sup>12,26</sup> The data presented in Figs. 1, 4, 9, and 10 cannot exclude, however, that the density of states at the Fermi level of the  $\text{LaH}_x$  compounds disappears only for  $x \approx 3$ .

#### IV. DISCUSSION

The NMR analysis of lanthanum hydrides  $\text{LaH}_x$ ,  $2 \leq x \leq 3$  yields detailed information on individual compounds and

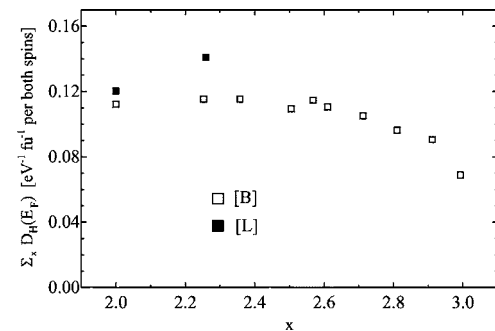


FIG. 10. Partial density of states at all proton sites in  $\text{LaH}_x$  as function of hydrogen concentration  $x$ , derived from proton Korringa relaxation rate, assuming  $s$ -like conduction electrons at the H site. [B]: Ref. 12, [L]: Refs. 26 and 29.

general information on the  $x$  dependence of the density of states. We will focus here on the latter aspect, since many structural details of  $\text{LaH}_x$  compounds have been analyzed before. We have shown in Sec. III, however, that homogeneous lattice distortion, hydrogen ordering phenomena, and hopping motion could be discussed based on  $^{139}\text{La}$  NMR results as well. We consider “integral” data first, and “local” information in Sec. IV B.

### A. Integral density of states as a function of hydrogen concentration

The Pauli paramagnetic susceptibility of conduction electrons can be converted into  $D_\chi(E_F)$  using

$$\chi_p = \mu_B^2 D_\chi(E_F). \quad (16)$$

The respective scale is given in Fig. 4 as well. The  $x$  dependence plotted for  $D_\gamma(E_F)$  in Fig. 1 and  $D_\chi(E_F)$  in Fig. 4 both are roughly linear, thus in general agreement. Due to the weak electron phonon coupling in  $\text{LaH}_2$ ,<sup>9</sup> it is permissible to assume that  $D_\gamma(E_F)$  reflects the bare density of states  $D_0(E_F)$  within 10% accuracy [ $D_\gamma(x=2) \approx 1.03$  versus  $D_0(x=2) = 0.912$  per eV, formula unit, both spins].  $D_\chi(E_F)$  derived with Eq. (16) is about a factor of 2.5 larger. In the simplifying discussion familiar for heavy-fermion systems this indicates a large degree of Coulomb correlations of the conduction electrons, which leads to the observed enhancement of the uniform magnetic susceptibility. As mentioned already in the Introduction a Wilson ratio  $R \approx 2.5$  would bring the lanthanum hydrides in close proximity to many typical heavy-fermion compounds.<sup>27</sup> We have to emphasize that this interpretation would be an oversimplification for the lanthanum hydrides. Due to the predominating  $d$ -like character of the density of states around the Fermi level of the lanthanum hydrides  $\text{LaH}_x$ ,  $2 \leq x \leq 3$ , an induced orbital or van Vleck contribution to the paramagnetic susceptibility  $\chi_p(x)$  of the conduction electrons must be considered in addition to the Pauli paramagnetic contribution in Eq. (16).<sup>36,47</sup> Even for simple cubic CsCl-structured La intermetallic compounds such as  $\text{LaAg}$  or  $\text{LaZn}$ , van Vleck contributions surpassing the  $s$  and  $d$  contributions by up to a factor of 4 were derived.<sup>52</sup> Thus the actual density of states will be lower than according to the right hand scale of Fig. 4.

### B. Local density of states and conduction electron character

Enhancement of the Korringa relaxation by Coulomb correlations is generally much weaker than the enhancement of the static magnetic susceptibility (or Knight shift), because all wave vectors are contributing instead of only  $q=0$  for the homogeneous field.<sup>53</sup> Thus local information about the density of states accessible via the Korringa contribution to proton ( $^1\text{H}$ ) and lanthanum ( $^{139}\text{La}$ ) spin lattice relaxation can be compared with  $D_0(E_F)$  or  $D_\gamma(E_F)$  reasonably well, even when neglecting enhancement factors.

We mentioned before that proton Korringa relaxation was considered to support a  $(3-x)^{1/3}$  dependence of the density of states.<sup>12</sup> The portion of the conduction electron density of states at the Fermi level that resides at the hydrogen sites is

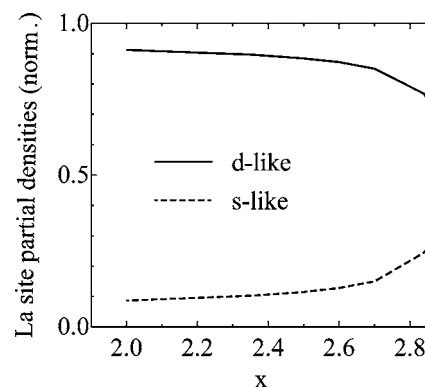


FIG. 11. Partial  $s$ - and  $d$ -like conduction electron density of states at the La site in  $\text{LaH}_x$ , derived from quantitative modeling of the spin-lattice relaxation rate [Eq. (18)].

relatively small, however. The published proton Korringa rates of  $\text{LaH}_x$  (Ref. 13) can be converted into local densities of states, using hydrogen  $s$ -electron hyperfine coupling  $\alpha_H(s) = 0.167$  MOe per electron.<sup>25,47</sup> Multiplied with the number of H atoms per formula unit,  $x$ , this total density of states around hydrogen sites  $\sum_x D_H$  is plotted in Fig. 10. The portion of the hydrogen centered density of states  $\sum_x D_H / D_0$  is only about 13% for  $\text{LaH}_2$ . In spite of the decrease of  $D_H(x)$  with  $x$  as  $(3-x)^{1/3}$ ,  $\sum_x D_H$  plotted in Fig. 10 is roughly constant with  $x$ , and the portion  $\sum_x D_H / D_0$  increases due to the decrease of  $D_0(x)$ , for  $2 < x < 2.8$ . Nevertheless, for  $x < 2.8$ , for the total density of states at the Fermi level clearly the predominant role is played by the lanthanum sites.

The Korringa relaxation rate for  $^{139}\text{La}$  in  $\text{LaH}_x$  is rather weak (Fig. 8) and the Knight shift  $K = (K + \Delta\sigma) - \Delta\sigma(\text{LaI}_3) = +(0.03 - 0.06)\%$  is almost zero for  $\text{LaH}_2$ . In agreement with the results of many band structure calculations that point to the prominent role of  $d$ -like conduction electrons in  $\text{RH}_x$ ,<sup>8</sup> we can therefore assume that  $^{139}\text{La}$  NMR reflects clearly the interplay of a large  $d$ -like and a small  $s$ -like portion of the conduction electron density of states at the La sites of  $\text{LaH}_x$ . Positive  $s$ -like and negative  $d$ -like (core polarization) contributions to the Knight shift almost cancel, if  $D_{\text{La}}^d \approx 10D_{\text{La}}^s$ , because the hyperfine coupling constants  $\alpha_d(\text{La}) \approx -0.1\alpha_s(\text{La})$  (with  $\alpha_s \approx 3.1$  MOe per spin).<sup>47</sup> Estimating the total La-site density of states via

$$D_{\text{La}} = D_{\text{La}}^s + D_{\text{La}}^d = D_0(E_F) - \sum_x D_H(E_F) \quad (17)$$

and fitting the  $^{139}\text{La}$  Korringa rates for neglected orbital contribution with

$$(T_1)_{ce}^{-1} = aT = \frac{1}{4} \pi \hbar \gamma_{\text{La}}^2 [(\alpha_s D_{\text{La}}^s)^2 + (\alpha_d D_{\text{La}}^d)^2] k_B T \quad (18)$$

gives the portions of  $s$ - and  $d$ -like density of states,  $D_{\text{La}}^s / D_{\text{La}}$  and  $D_{\text{La}}^d / D_{\text{La}}$ , plotted in Fig. 11. About 90% of the La-site partial density of states is  $d$ -like in character, and only 10%  $s$ -like, according to this model analysis. There is only a weak  $x$  dependence of this decomposition. The relative role of both contributions is in fair agreement with the very detailed band structure calculational results for  $\text{YH}_2$  published recently<sup>36</sup> or with earlier interpretation of  $\text{LaH}_2$  results by the same

authors.<sup>35</sup> Along the same lines, the Knight shift for the  $^{139}\text{La}$  nucleus in  $\text{LaH}_2$  can be estimated, considering as limiting value the enhancement of the static magnetic susceptibility by a factor of 2.5 derived in Sec. IV A. The calculated value  $K_{s+d} = +0.025\%$  is in surprising agreement with the experimental value estimated as  $K \approx (K + \Delta\sigma) - \Delta\sigma(\text{LaI}_3) = +(0.03 - 0.06)\%$  in Secs. III D 1 and III D 2, above. It is clear that the orbital contribution, calculated in Ref. 36 for the  $\text{YH}_2$  dihydride and expected for  $\text{LaH}_x$  as well, will give a positive line shift contribution entering in the resulting  $(K + \Delta\sigma)$  as well. The decrease of the portion of  $d$ -like density of states at the La site with  $x$ , shown in Fig. 11, explains also the apparent contradiction between the linear variation of the density of states information from La Korringa rate, and the clearly nonlinear variation of the corresponding information deduced from  $\text{Gd}^{3+}$  electron spin Korringa rate: hyperfine interaction reflects the  $s$  part of the density by a factor of 10 more sensitive than the  $d$  part, but for  $4f$ -conduction electron exchange interaction it is just the other way around

## V. CONCLUSIONS

We presented a detailed analysis of the electronic structure of lanthanum hydrides  $\text{LaH}_x$ , based primarily on low-temperature  $^{139}\text{La}$  NMR investigations. We discussed the role of electron-electron correlations by considering that the paramagnetic susceptibility of the conduction electrons is enhanced by about 2.5 compared to the bare value of Pauli paramagnetism. We pointed, however, to the fact that these increased  $\chi_p$  values can originate from van Vleck type induced orbital contributions, at least in part. We analyzed the structural influence on  $^{139}\text{La}$  NMR spectra and derived the variation of the  $^{139}\text{La}$  NMR line shift with temperature and hydrogen concentration. Chemical shift is a relevant part of the line shift. Thus the Knight shift can not reliably be separated for varied hydrogen content from the chemical shift variation. We showed that spin-lattice relaxation can be quantitatively analyzed for  $^{139}\text{La}$  in  $\text{LaH}_x$  compounds in spite

of local electric field gradients and only partial access to the wide spectra. The  $x$  dependence of the La-site-specific conduction electron density of states at the Fermi level has thus been derived. Combined analysis of proton and  $^{139}\text{La}$  spin lattice relaxation and  $x$ -dependent total density of states proves the predominant  $d$ -like character of conduction electrons at the La site. Most generally,  $D_\gamma(E_F)$ ,  $D_\chi(E_F)$ , and  $^{139}\text{La}$ -relaxation point to an almost linear  $x$  dependence of the density of states at the Fermi level in  $\text{LaH}_x$ ,  $2 \leq x \leq 3$ , in contrast to the more nonlinear variation already reported for the hydrogen site long ago, and the lanthanum site according to Gd electron spin Korringa relaxation in  $\text{LaH}_x$ , reported recently. All the low-temperature results for various degrees of H ordering in the  $\text{LaH}_x$  series  $2 \leq x \leq 3$  can only be reconciled by taking the varying spatial distribution of  $s$  and non- $s$  characters of the conduction electrons into account. We did not focus on charge transport and the metal-semiconductor transition, related to the order/disorder transition of the H atoms on the octahedral interstitial sites (and concomitant low- $T$  overall lattice distortion) in the temperature range above 200 K for  $2.7 < x < 2.9$ . Critical temperatures and a critical concentration might be derived based on these phenomena. Instead, this investigation is focused on the  $x$  dependence of the electronic density of states at the Fermi level. The variation of the low temperature integral or local conduction electron densities of states of the lanthanum hydrides  $\text{LaH}_x$  with  $x$  varying between 2 and 3 appears less peculiar considering the additional data presented above.

## ACKNOWLEDGMENTS

We thank U. Eberle, G. Fischer, and G. Majer for experimental contributions. Ames Laboratory is operated for the U.S. Department of Energy by Iowa State University under Contract No. W-7405-Eng-82. This work was supported by the Director of Energy Research, Office of Basic Energy Sciences. We thank the Deutsche Forschungsgemeinschaft for financial support (Grant No. Do 181/12).

\*Electronic address: elmar.dormann@pi.uka.de

- <sup>1</sup>R. R. Arons, in *Rare earth hydrides*, Landolt-Börnstein, New Series, Group III (Springer, Berlin, 1991), Vol. 19d1, p. 280.
- <sup>2</sup>P. Vajda, *Handbook on the Physics and Chemistry of Rare Earths*, edited by K. A. Gschneider, Jr. and L. Eyring (Elsevier, Amsterdam, 1995), Vol. 20, Chap. 137.
- <sup>3</sup>R. G. Barnes, *Topics in Applied Physics*, edited by H. Wipf (Springer, Berlin, 1997), Vol. 73, p. 93.
- <sup>4</sup>K. Kai, K. A. Gschneidner, Jr., B. J. Beaudry, and D. T. Peterson, *Phys. Rev. B* **40**, 6591 (1989).
- <sup>5</sup>B. Stalinski, *Bulletin de l'Académie Polonaise des Sciences* **V**, 997 (1957).
- <sup>6</sup>B. Stalinski, *Bulletin de l'Académie Polonaise des Sciences* **V**, 1001 (1957).
- <sup>7</sup>J. N. Huiberts, R. Griessen, J. H. Rector, R. J. Wijngaarden, J. P. Dekker, D. G. deGroot, and N. J. Koeman, *Nature (London)* **380**, 231 (1996).
- <sup>8</sup>A. T. M. van Gogh, D. G. Nagengast, E. S. Kooij, N. J. Koeman, J. H. Rector, R. Griessen, C. F. J. Flipse, and R. J. J. G. A. M. Smeets, *Phys. Rev. B* **63**, 195105 (2001).
- <sup>9</sup>M. Gupta, J. P. Burger, *Phys. Rev. B* **22**, 6074 (1980).
- <sup>10</sup>R. G. Barnes, B. J. Beaudry, D. R. Torgeson, C. T. Chang, and R. B. Creel, *J. Alloys Compd.* **253-254**, 445 (1997).
- <sup>11</sup>J. Shinar, B. Dehner, R. G. Barnes, and B. J. Beaudry, *Phys. Rev. Lett.* **64**, 563 (1990).
- <sup>12</sup>R. G. Barnes, C. T. Chang, G. Majer, and U. Kaess, *J. Alloys Compd.* **356-357**, 137 (2003).
- <sup>13</sup>R. G. Barnes, C. T. Chang, M. Belhoul, D. R. Torgeson, R. J. Schoenberger, B. J. Beaudry, and E. F. W. Seymour, *J. Less-Common Met.* **172-174**, 411 (1991).
- <sup>14</sup>R. G. Barnes, B. J. Beaudry, R. B. Creel, D. R. Torgeson, and D. G. de Groot, *Solid State Commun.* **36**, 105 (1980).
- <sup>15</sup>O. J. Zogal, C. Juszczak, A. H. Vuorimäki, E. E. Ylinen, M. Punkkinen, and H. Drulis, *J. Alloys Compd.* **191**, 207 (1993).

- <sup>16</sup>Z. Bieganski, D. Gonzales Alvarez, and F. W. Klaaijzen, *Physica* (Amsterdam) **37**, 153 (1967).
- <sup>17</sup>Z. Bieganski and M. Drulis, *Phys. Status Solidi A* **44**, 91 (1977).
- <sup>18</sup>Z. Bieganski and B. Stalinski, *Z. Phys. Chem., Neue Folge* **116**, 109 (1979).
- <sup>19</sup>E. Boroch, K. Conder, Cai Ru-Xiu, and E. Kaldis, *J. Less-Common Met.* **156**, 259 (1989).
- <sup>20</sup>T. J. Udovic, Q. Huang, J. J. Rush, J. Schefer, and I. S. Anderson, *Phys. Rev. B* **51**, 12 116 (1995).
- <sup>21</sup>T. J. Udovic, Q. Huang, and J. J. Rush, *J. Solid State Chem.* **122**, 151 (1996).
- <sup>22</sup>T. J. Udovic, Q. Huang, and J. J. Rush, *Phys. Rev. B* **61**, 6611 (2000).
- <sup>23</sup>D. L. Schreiber and R. M. Cotts, *Phys. Rev.* **131**, 1118 (1963).
- <sup>24</sup>G. Majer, U. Kaess, and R. G. Barnes, *Phys. Rev. Lett.* **83**, 340 (1999).
- <sup>25</sup>A. Abragam, *Principles of Nuclear Magnetism* (Clarendon, Oxford, 1961).
- <sup>26</sup>S. Leyer, R. G. Barnes, C. Buschhaus, G. Fischer, B. Pilawa, B. Pongs, A. Tinner, and E. Dormann, *J. Phys.: Condens. Matter* **16**, 6147 (2004), and references therein.
- <sup>27</sup>H. v. Löhneysen, *J. Magn. Magn. Mater.* **200**, 532 (1999).
- <sup>28</sup>S. Leyer and E. Dormann, *J. Alloys Compd.* **363**, 15 (2004).
- <sup>29</sup>S. Leyer, J. Weizenecker, and E. Dormann, *J. Phys.: Condens. Matter* **12**, 6927 (2000).
- <sup>30</sup>E. Fukushima and S. B. W. Roeder, *Experimental Pulse NMR, a Nuts and Bolts Approach* (Addison-Wesley, Reading, MA, 1981).
- <sup>31</sup>A. Narath, *Phys. Rev.* **162**, 320 (1967).
- <sup>32</sup>S. Leyer, Ph.D. thesis, Universität Karlsruhe, Karlsruhe, 2004.
- <sup>33</sup>P. Vajda, J. P. Burger, and J. N. Daou, *J. Phys.: Condens. Matter* **3**, 6267 (1991).
- <sup>34</sup>P. W. Sellwood, *Magnetochemistry* (Interscience, New York, 1956), p. 78.
- <sup>35</sup>O. J. Zogal and B. Nowak, *Z. phys. Chem.* **181**, 43 (1993).
- <sup>36</sup>B. Jäger, P. Herzog, W. Wolf, B. Nowak, and O. J. Zogal, *Solid State Commun.* **130**, 215 (2004).
- <sup>37</sup>S. Heck, diploma thesis, Universität Karlsruhe, Karlsruhe, 2004.
- <sup>38</sup>P. Klavins, R. N. Shelton, R. G. Barnes, and B. J. Beaudry, *Phys. Rev. B* **29**, 5349 (1984).
- <sup>39</sup>M. Mehring, *High Resolution NMR Spectroscopy in Solids* (Springer, Berlin, 1976).
- <sup>40</sup>X. Helluy, J. Kümmerlen, A. Sebald, and O. J. Zogal, *Solid State Nucl. Magn. Reson.* **14**, 225 (1999).
- <sup>41</sup>A. Sebald, in *NMR Basic Principles and Progress*, edited by B. Blümich (Springer-Verlag, Berlin, 1994), Vol. 31, p. 91.
- <sup>42</sup>A. Kaiser, and E. Dormann, *Phys. Rev. B* **71**, 115108 (2005).
- <sup>43</sup>A. L. Allred and E. G. Rochow, *J. Inorg. Nucl. Chem.* **5**, 264 (1958).
- <sup>44</sup>L. Eyring, *Handbook on the Physics and Chemistry of Rare Earths*, edited by K. A. Gschneidner, Jr. and L. Eyring (North Holland, Amsterdam, 1979), Vol. 3, p. 337.
- <sup>45</sup>J. M. Haschke, in *Handbook on the Physics and Chemistry of Rare Earths* (Ref. 44), Vol. 4, p. 89.
- <sup>46</sup>W. T. Carnall, in *Handbook on the Physics and Chemistry of Rare Earths* (Ref. 44), Vol. 3, p. 171.
- <sup>47</sup>E. Dormann, in *Handbook on the Physics and Chemistry of Rare Earths*, edited by K. A. Gschneidner, Jr. and L. Eyring (North Holland, Amsterdam, 1991), Vol. 14, Chap. 94, p. 63.
- <sup>48</sup>A. H. Vuorimäki, E. E. Ylinen, B. Nowak, and O. J. Zogal, *Solid State Commun.* **122**, 469 (2002).
- <sup>49</sup>J.-W. Han, C.-T. Chang, D. R. Torgeson, E. F. W. Seymour, and R. G. Barnes, *Phys. Rev. B* **36**, 615 (1987).
- <sup>50</sup>M. Jerosch-Herold, L.-T. Lu, D. R. Torgeson, D. T. Peterson, R. G. Barnes, and P. M. Richards, *Z. Naturforsch. B* **40**, 222 (1985).
- <sup>51</sup>A. Abragam and B. Bleaney, *Electron Paramagnetic Resonance of Transition Ions* (Clarendon, Oxford, 1970), p. 553.
- <sup>52</sup>U. Goebel, E. Dormann, and K. H. J. Buschow, *J. Phys. F: Met. Phys.* **5**, 2198 (1975).
- <sup>53</sup>A. Narath, *Phys. Rev.* **179**, 359 (1969).